Experimental Layered/Enhanced ACO-OFDM short-haul optical fiber link

Binhuang Song, Chen Zhu, Bill Corcoran, *member, IEEE*, Qibing Wang, Leimeng Zhuang, *member, IEEE* and Arthur J. Lowery, *Fellow, IEEE*

***Abstract*— Asymmetrically clipped optical orthogonal frequency division multiplexing (ACO-OFDM) is theoretically more optically power efficient than DC-biased OFDM (DCO-OFDM); unfortunately its spectral efficiency is halved to accommodate the clipping distortion. Recently, Layered/Enhanced ACO-OFDM has been developed to mostly regain the lost spectral efficiency, and theoretically compared with other modulation formats. In this letter, we experimentally demonstrate L/E-ACO-OFDM for the first time over a fiber link. We transmit over a 19.8-km single mode fiber at 4.375 Gbits/s, and show a 2-dB improvement in signal quality for the same laser bias current and received optical power over DCO-OFDM.**

***Index Terms*— intensity modulation with direct detection (IM/DD), asymmetrically clipped orthogonal frequency division multiplexing (ACO-OFDM), optical communication.**

I. Introduction

SHORT-haul optical fiber communication links usually adopt low-cost solutions such as intensity modulation with direct detection (IM/DD). IM/DD requires positive-valued modulation formats, such as: pulse amplitude modulation (PAM) [1], discrete multi-tone (DMT) or DCO-OFDM [2],[3], and ACO-OFDM [4],[5]. DMT/OFDM provide higher spectral efficiencies than PAM, for a given optical power, and are less sensitive to dispersion-induced power fading if bit and/or power loading are used [6]. DCO-OFDM guarantees non-negative signals by adding an adequate bias: ACO-OFDM simply sets all negative values to zero—asymmetric clipping—causing distortion tones, which can be allocated to unused "even" subcarriers [5], thereby sacrificing half the spectral efficiency. To regain the spectral efficiency, hybrid DCO/ACO-OFDM technology has been proposed in [7]. Layered (or Enhanced) ACO-OFDM is an alternative way to increase spectral efficiency of ACO-OFDM [8],[9], whilst still retaining most of its power efficiency. Alternatively, SEE-OFDM [10], and Enhanced-Unipolar-OFDM [11] also provide similar methods to enhance flip/unipolar OFDM [12],[13]. Augmented PAM-DMT [14] similarly enhances PAM-DMT. All of these methods start with a clipped signal whose distortion falls away from itself (Layer 1), for example on even subcarriers. At the receiver, this signal can be recreated, so its distortion subtracted. In L/E-ACO-OFDM this subtraction enables additional signals carried on half of the even subcarriers (Layer 2), and be received and decoded substantially without interference. Once the Layer 2 signal has been decoded, its interference can be cancelled, enabling signals to be received on half of the remaining even subcarriers (Layer 3). Simulations at high constellation sizes have shown that these methods provide better signal qualities at lower optical powers than DCO-OFDM, but have spectral efficiencies approaching DCO-OFDM [15]. This implies that optical sources, such as lasers, can be operated at lower bias currents and output powers. Looked at another way, a given laser would be able to provide a higher modulated optical power, so be transmitted further.

In order to have a reasonable frequency response and low transient distortion, however, a direct modulated laser (DML) must be biased somewhat above its threshold current [16]. This could reduce the power efficiency advantage of an L/E-ACO-OFDM signal, because the laser spends more time at low powers (that is, during the times the signal is asymmetrically clipped) than when driven by DCO-OFDM signals (which have infrequent and short-duration zero-level clipping), and hence is slow to turn back on. A post-equalizer could partially compensate this distortion.

This letter provides the first experimental demonstration of L/E–ACO-OFDM and a comparison with DCO-OFDM in a short-haul optical fiber link. We used a truncated second-order Volterra filter to equalize the DCO-OFDM and the L/E-ACO-OFDM signals. A noise cancellation algorithm was also implemented for L/E-ACO-OFDM. Our results show that, for the same laser bias current and output power, L/E-ACO-OFDM provides up to 3.8-dB sensitivity improvement over DCO-OFDM for back-to-back transmission and a 2-dB advantage after 19.8-km of standard single-mode fiber.

II. Waveform Generation

Real-valued waveforms for DCO-OFDM and L/E-ACO-OFDM systems can be generated by allocating complex data and its Hermitian conjugate value to positive and negative

This work is supported under the Australian Research Council's Laureate Fellowship (FL130100041) and CUDOS – ARC Centre of Excellence for Ultrahigh bandwidth Devices for Optical Systems (CE110001018).

Binhuang Song, Chen Zhu, Bill Corcoran, Qibing Wang, Leimeng Zhuang and Arthur J. Lowery are with the Department of Electrical and Computer Systems Engineering, Monash University, Melbourne, VIC 3800, Australia. Chen Zhu is now with Bell Laboratories, Nokia, 600 Mountain Ave, Murray Hill, NJ 07974, USA. (e-mail: binhuang.song@monash.edu; chen.zhu@nokia.com; bill.corcoran@monash.edu;qibing.wang@monash.edu; leimeng.zhuang@monash.edu; arthur.lowery@monash.edu).

frequency sub-carriers before the inverse Discrete Fourier transforms (IDFT). For DCO-OFDM signals, a strong DC bias is added to minimize excursions below zero, as shown in Fig. 1(b). In L/E-ACO-OFDM, the signal generated for each Layer (or Chord [15]) has its negative values clipped to zero, before being combined with the signals of the other layers. The frequency allocations of the signals in each Layer are such that the clipping distortion from Layer n only falls upon Layer (n+1), enabling the received signal to be iteratively decoded, starting with Layer 1.

To be more specific, instead of loading data to all positive half of the IDFT size sub-carriers directly (in Fig. 1(a)), we load 1st-layer ACO-OFDM data to red sub-carriers (index 1+2n, n = 0,1,2,…5), the 2nd-layer ACO-OFDM data to green sub-carriers (index 2+4n, n = 0,1,2), then the 3rd ACO-OFDM data to purple sub-carriers (index 4+8n, n = 0,1) as in Fig. 1(c). Then all negative values are set to zero before three layers' waveforms are superposed as in Fig. 1(d). To decode data in the receiver side, the 1st-layer will be first processed with a forward FT as it does not any suffer clipping noise from other layers, then its clipping noise (red stars in Fig. 1(f)) is estimated and removed before processing the next layer.

III. Receiver Algorithms

Conventionally, a bank of one-tap frequency domain equalizers are used for OFDM signals, one for each subcarrier. However, in this experiment, to compensate the laser distortion, a Volterra filter time-domain equalizer is implemented in the receiver.

A. Truncated second-order Volterra filter

Volterra filters have been used to compensate chromatic dispersion-induced and chirp-induced distortions in optical communication systems, and nonlinear distortion in high power amplifiers in wireless systems [3],[17],[18]. Because of the square-law detection in an IM/DD system, a second-order Volterra filter most suitable. An output, y, of a truncated Volterra filter is:

$$y(k)=\sum_{l_1=0}^{L-1} w_1(l_1)x(k-l_1)+\sum_{l_1=0}^{L-1}\sum_{l_2=0}^{L-1} w_2(l_1,l_2)x(k-l_1)x(k-l_2) \quad (1)$$

where: x is the input signal; w_1 and w_2 are weights for linear and second-order terms. Eqn. (1) is a linear finite impulse response (FIR) filter with L taps plus a second-order FIR filter with $L(L+1)/2$ taps. The second term operates on the cross-products between different samples, x_k. By considering the memory length of the channel and computing complexity, we chose L=10 for this experiment. A training sequence with a least-mean-square (LMS) algorithm is used to update the weights. This time domain equalizer can deal with arbitrary modulation formats, as it only performs waveform correction.

B. Noise cancellation algorithm for L/E-ACO-OFDM

For the L/E-ACO signals, after time-domain Volterra equalization, an iterative noise cancellation algorithm further reduces the noise transfer between different layers. The algorithm is similar to [19], which takes advantage of anti-symmetric property of ACO-OFDM waveforms. For example, the values of a1 and a1' (shown in Fig. 2) are compared and the smaller one is set to zero; this removes up to half of the noise power.

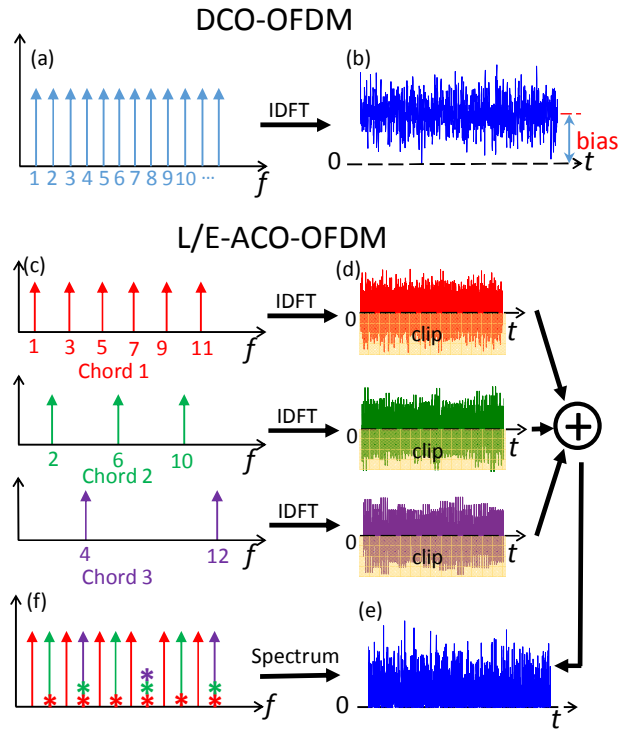

Fig. 1. (a) Frequency-domain and (b) time-domain conceptual diagrams for DCO-OFDM, (Arrows: sub-carriers). (c) Frequency-domain and (d) time-domain conceptual diagrams for each layer/chord in L/E-ACO-OFDM. (e) Time-domain and (f) frequency domain conceptual diagrams for total L/E-ACO-OFDM (Arrows: sub-carriers, star symbols: clipping noise).

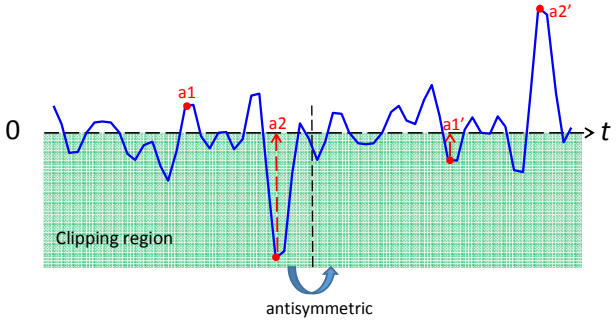

Fig. 2. Waveform of single layer/chord in L/E-ACO-OFDM. Blue trace: ACO-OFDM waveform before clipping. Any value in the green region will be clipped to zero. Before clipping, point a1 (a2) has same magnitude as a1' (a2') but with the opposite sign.

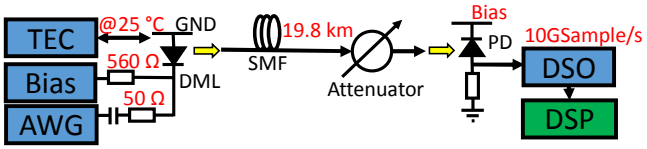

Fig. 3. Experimental setup. DSP: off-line digital single processing. AWG: arbitrary waveform generator. DML: direct modulated laser. TEC: temperature controller. SMF: single mode fiber. PD: photodetector. DSO: digital oscilloscope.

IV. Experiments

Figure 3 shows the experimental setup for 4.375-Gb/s QPSK transmission using DCO and L/E-ACO. The DCO signal was

generated in MATLAB with 256-point FFT, and has 63 data sub-carriers with the 1st sub-carrier left for DC bias. For L/E-ACO, we stack 3 layers (chords) with the same FFT size and oversampling rate, carrying 32, 16 and 8 sub-carriers for the 1st, 2nd and 3rd layers. The L/E-ACO's spectral efficiency is 87.5% ((32+16+8)/64) of DCO. In MATLAB, both the L/E-ACO and DCO signals were normalized, so that their per-subcarrier electrical powers are identical. Then the DCO signal was clipped at 4-sigma before being mapped into a +/- 0.5-V range to suit a Tektronix 7102 arbitrary waveform generator (AWG). The same scaling factor was applied for L/E-ACO. Thus, because of the 50-Ω impedance of the laser and series resistor, both drive signals have 20-mA p-p amplitudes. The laser was a Gooch & Housego AA0701 DFB, controlled to 25℃. To achieve identical bit rates, the AWG set to 8.75 Gsample/s for DCO and 10 Gsample/s for L/E-ACO. This increases the signal bandwidth of L/E-ACO; however, the bandwidth is expected to be very close to DCO when more layers are used. The output of a 13-GHz photodiode was sampled by a 28-GHz real-time digital oscilloscope (Agilent DSO-X92804A) at 10 GSample/s.

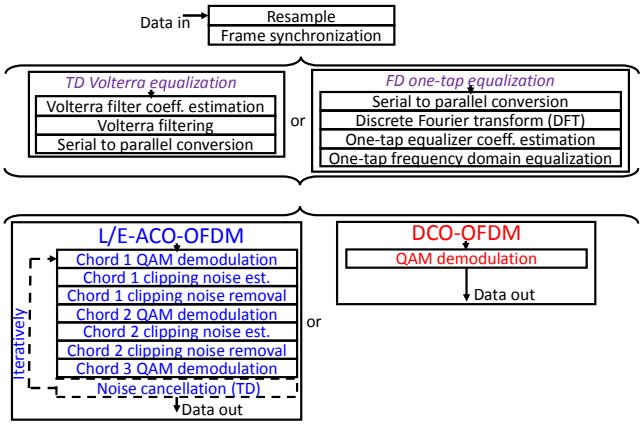

Fig. 4. Receiver DSP flowchart. Either time-domain Volterra equalization (left purple) and frequency-domain one-tap equalizing (right purple) are applied on L/E-ACO-OFDM (blue) and DCO-OFDM (red).

Figure 4 shows the receiver DSP. For both systems, we use either frequency-domain one-tap equalization or time-domain Volterra equalization (with noise cancellation for L/E-ACO). For each transmission situation, we plotted the *Q*-factor for a range of bias currents.

V. Results and Discussion

We first performed a back-to-back transmission experiment without Volterra equalization. Firstly, we removed the attenuator and identified the optimal bias (20.95 mA for L/E-ACO and 21.07 mA for DCO). Fig. 5 plots the measured *Q*-factors versus attenuation. In the higher-attenuation region, where the thermal noise (electrical noise) of the receiver dominates over the signal distortion, the *Q*-factor drops 2-dB for every 1-dB increase in attenuation, as expected. At low attenuations, the *Q*-factor is limited by system imperfections such as quantization noise in the AWG and oscilloscope.

We next studied the effect of bias current on a back-to-back system, with the attenuation set to zero. As shown in Fig. 4 we used either TD Volterra equalization or FD equalization for both types of OFDM. Additionally, when using TD Volterra equalization and L/E-ACO, we also used noise cancellation. Fig. 6 shows that for biases below 19 mA L/E-ACO outperforms DCO, and TD Volterra equalization improves both

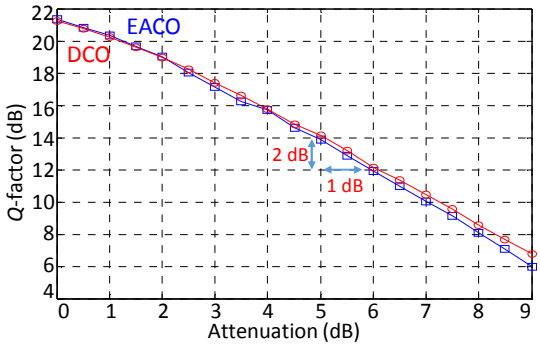

Fig. 5. *Q*-factor versus attenuation for L/E-ACO-OFDM (blue squares) and DCO-OFDM (red circles).

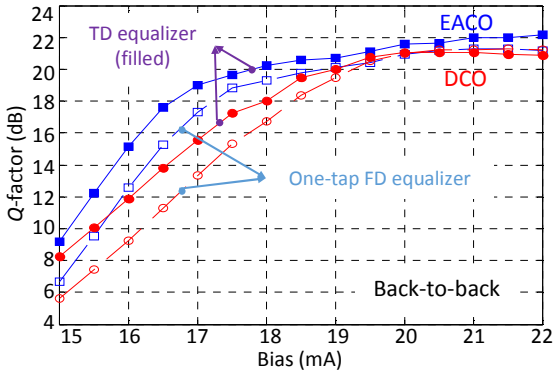

Fig. 6. Back-to-back *Q*-factor versus different bias for L/E-ACO-OFDM (blue line with squares) and DCO-OFDM (red line with circles). Solid line with filled symbols: using time domain equalizer. Dashed line with clear symbols: using frequency domain one-tap equalizer.

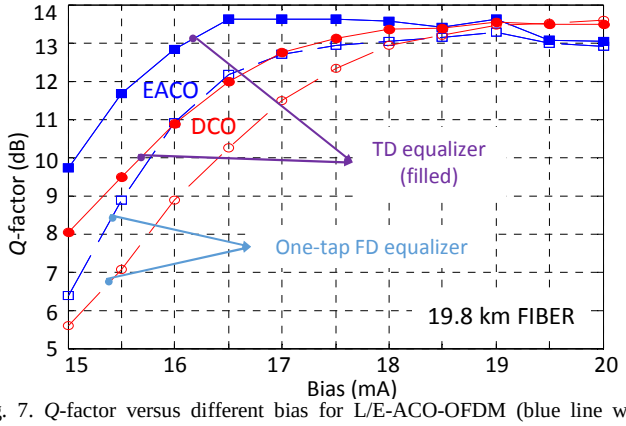

Fig. 7. *Q*-factor versus different bias for L/E-ACO-OFDM (blue line with circles) and DCO-OFDM (red line with diamonds) after 19.8-km optical fiber transmission. Solid line with filled symbols: using time domain equalizer. Dashed line with clear symbols: using frequency domain one-tap equalizer.

of the OFDM systems. At 17-mA bias the *Q*-factor of TD-equalized L/EACO is 3.8-dB better than TD-equalized DCO. At high biases (>20 mA), the system is limited by other factors, such as quantization noise.

Lastly, we compared the *Q*-factors for two OFDM formats in a 19.8-km single-mode fiber short-haul link. Due to the low accumulated dispersion, we did not use a cyclic prefix (CP) nor

bit/power loading. Fig. 7 plots the measured *Q*-factors at different laser bias currents. Similarly to the back-to-back results, the Volterra equalizer improves the signal quality for both OFDM formats. At 16-mA bias, L/E-ACO achieves a 2-dB *Q*-factor improvement over DCO. At high biases, the signal quality is reduced below the back-to-back case by ISI, from a combination of laser chirp, fiber dispersion, and fiber loss.

To transmit signals with the same AC-modulated optical power, L/E-ACO requires less DC bias than DCO, so operates at lower mean optical powers. Some simple calculations of biases required for no laser clipping reveal the reason. For the L/E-ACO signal, the mean level of the AWG output was measured to be 18% of its peak-to-peak output [15]. The AWG output is 1-V peak-peak, giving mean drive current level of a 20×0.18 = 3.6 mA. As a DC-block removes this mean level, the laser should be biased at >3.6 mA above the laser's threshold of 12.4 mA, that is, >16 mA. For DCO, a bias of 20/2 = 10 mA above threshold (giving 22.4 mA) is required to eliminate any clipping due to the laser. Thus, L/E-ACO should require 6.4-mA less bias than DCO.

For the fiber experiment, the bias currents to maintain the *Q*-factors above 13 dB were 16.5 mA (L/E-ACO) and 18 mA (DCO), equivalent to 4.1 mA and 5.6 mA above threshold. This indicates that the L/EACO requires 0.5-mA more bias than expected from the simple calculation above; probably because the L/EACO waveform is close to its minimum value for a reasonable proportion (approx. 0.5^3 = 12.5%) of an OFDM symbol due to the independent clipping-at-zero of the three Layers, so the laser is more likely to suffer from transient distortion and low modulation bandwidths. The DCO system is biased lower than the calculated value that eliminates laser clipping, simply because fiber effects limit the advantage of increasing the bias further. That said, L/E-ACO saves (5.6-4.1)/5.6 = 27% of the bias current in excess of the threshold current, compared with DCO. Greater advantages are also expected for higher constellation sizes [15], though laser dynamics may reduce this advantage. With a directly modulated laser, a reduced bias translates to a lower average optical power. More energy efficiency can be expected for a laser with a lower threshold and less nonlinear distortion—a potential candidate is a vertical-cavity surfacing-emitting laser (VCSEL), which normally have wider bandwidths and lower thresholds [20]. Higher-order Volterra filters could further improve the signal quality [21]. Such a solution could be useful for future green optical communications, where the energy consumption is critical [22].

VI. Conclusion

In this letter, we have reported the first short-haul optical fiber transmission experiment using L/E–ACO-OFDM. The experimental results shows that L/E–ACO-OFDM can have a 3.8-dB and 2-dB Q-factor advantage over DCO-OFDM in back-to-back transmission and over 19.8-km of optical fiber, respectively. Volterra-filter based time-domain equalizers considerably improve both of the OFDM systems.

References

[1] S. Zhou, X. Li, L. Yi, Q. Yang and S. Fu, "Transmission of 2×56 Gb/s PAM-4 signal over 100 km SSMF using 18 GHz DMLs," *Opt. Lett.*, vol. 21, no. 8, pp. 1805-1808, 2016.

[2] S. C. Lee, S. Randel, F. Breyer and A. M. Koonen, "PAM-DMT for intensity-modulated and direct-detection optical communication systems," *IEEE Photon. Technol. Lett.*, vol. 21, no.23, pp 1749-1751, Dec. 2009.

[3] W. Yan, B. Liu, L. Li, Z. Tao, T. Takahara and J. C. Rasmussen, "Nonlinear distortion and DSP-based compensation in metro and access networks using discrete multi-tone," in *Proc. ECOC*, Amsterdam, Sept. 2012, paper Mo-1.

[4] A. J. Lowery and J. Armstrong, "10 Gbit/s multimode fiber link using power-efficient orthogonal-frequency division multiplexing," *Opt. Exp.*, vol. 13, no. 25, pp. 10003–10009, 2005.

[5] J. Armstrong and A. J. Lowery, "Power efficient optical OFDM," *Electron. Lett.*, vol. 42, no. 6, pp. 370-372, 2006.

[6] Q. Zhang, Y. Fang, E. Zhou, T. Zuo, L. Zhang, G. N. Liu and X. Xu, "C-band 56Gbps transmission over 80-km single mode fiber without chromatic dispersion compensation by using intensity-modulation direct-detection," in *Proc. ECOC*, Cannes, Sep. 2014, paper P.5.19.

[7] S. D. Dissanayake and J. Armstrong, "Comparison of ACO-OFDM, DCO-OFDM and ADO-OFDM in IM/DD Systems," *J. Lightwave Technol.*, vol. 31, no. 7, pp. 1063-1072, 2013.

[8] M. Islim, D. Tsonev, and H. Haas, "On the superposition modulation for OFDM-based optical wireless communication," in *Proc. IEEE Global Signal and Information Processing conference*, 2015, pp. 1022–1026.

[9] Q. Wang, C. Qian, X. Guo, Z. Wang, D. G. Cunningham, and I. H. White, "Layered ACO-OFDM for intensity modulated direct-detection optical wireless transmission," *Opt. Exp.*, vol. 23, no. 9, pp. 12382–12393, 2015.

[10] H. Elgala and T. Little, "SEE-OFDM: spectral and energy efficient OFDM for optical IM/DD systems," in *Proc. IEEE Personal, Indoor, and Mobile Radio Communication*, 2014, pp. 851–855.

[11] D. Tsonev, S. Videv, and H. Haas, "Unlocking spectral efficiency in intensity modulation and direct detection systems," *IEEE J. Sel. Areas Commun.*, Vol. 33, no. 9, pp. 1758–1770, 2015.

[12] N. Fernando, Y. Hong, and E. Viterbo, "Flip-OFDM for unipolar communication systems," *IEEE Trans. on Commun.*, Vol. 60, no. 12, pp. 3726–3733, 2012.

[13] D. Tsonev, S. Sinanovic, and H. Haas, "Novel unipolar orthogonal frequency division multiplexing (U-OFDM) for optical wireless," in *Proc. of IEEE Vehicular Technology Conference*, 2012, pp. 1–5.

[14] M. S. Islim and H. Haas, "Augmenting the spectral efficiency of enhanced PAM-DMT-based optical wireless communications," *Opt. Exp.*, Vol. 24, no. 11, pp. 11932-11949, 2016.

[15] A. J. Lowery, "Comparisons of spectrally-enhanced asymmetrically-clipped optical OFDM systems," *Opt. Exp.*, vol. 24, no. 4, pp. 3950-3966, 2016.

[16] R. S. Tucker, "High-speed modulation of semiconductor lasers," *IEEE Trans. Electron Devices*, vol. 32, no. 12, pp. 2572–2584, Dec. 1985.

[17] N. S. André, K. Habel, H. Louchet and A. Richter, "Adaptive nonlinear Volterra equalizer for mitigation of chirp-induced distortions in cost effective IMDD OFDM systems," *Opt. Exp.*, vol. 21, no. 22, pp. 26527-26532, 2013.

[18] A. Zhu and T. J. Brazil, "Behavioral modeling of RF power amplifiers based on pruned Volterra series," *Microwave and Wireless Components Lett.*, vol. 14, no. 12, pp. 563-565, 2004.

[19] Q. Wang, Z. Wang, X. Guo and L. Dai, "Improved receiver design for layered ACO-OFDM in optical wireless communications," *IEEE Photon. Technol. Lett.*, vol. 28, no.3, pp 319-322, Oct. 2015.

[20] E. Haglund *et al.*, "High-speed VCSELs with strong confinement of optical fields and carriers," *J. Lightwave Technol.*, vol. 34, no. 2, pp. 269 - 277, 2015.

[21] H. Y. Chen *et al.*, "52.5% data rate improvement by employing Volterra filtering and exponential companding in a high loss budget and high-capacity OFDM long-reach PON," in *Proc. OFC*, Anaheim, CA, USA, Mar. 2016, pp. 1–3, paper Th3C.3.

[22] R. S. Tucker, "Green optical communications—Part II: Energy limitations in networks," *IEEE J. of Sel. Quantum Electronics*, vol. 17, no. 2, pp. 261-274, 2011.